Lasing in a random amplifying medium: Spatiotemporal characteristics and nonadiabatic atomic dynamics

Lucia Florescu and Sajeev John
Department of Physics, University of Toronto, 60 St. George Street, Toronto, Ontario, Canada M5S 1A7
(Received 3 September 2003; published 20 September 2004)

We study the dynamics of lasing from photonic paints excited by short, localized, optical pulses, using a time-dependent diffusion model for light propagating in the medium containing active atoms. The full time-dependent, nonadiabatic nonlinear response of the atomic system to the local optical field intensity is described using the Einstein rate equations for absorption and emission of light. Solving the time-dependent diffusion equation for the light intensity in the medium with nonlinear gain and loss, we derive detailed information on the spectral, spatial, and temporal properties of the emitted laser light. Our model recaptures the effects of scatterers to narrow the emission spectral linewidth and to narrow the emitted pulse duration, at a specific threshold pump intensity. Our model also describes how this threshold pump intensity decreases with scatterer density and excitation spot diameter, in excellent agreement with experimental results.

DOI: 10.1103/PhysRevE.70.036607 PACS number(s): 42.25.Dd, 42.55.Zz, 42.60.Da

I. INTRODUCTION

In conventional lasers, lasing is achieved by positive feedback. The radiation emitted and redirected into the active medium stimulates further emission, which reinforces the propagating field. The excitation threshold for coherent emission is reached when the gain in a round trip exceeds the loss. This can lead to a coherent mode, which builds up inside the cavity. Part of this light is coupled out of the cavity to form a unidirectional monochromatic beam.

Weak scattering of light has traditionally been considered detrimental to laser action, since such scattering removes photons from the lasing mode of a conventional cavity. On the other hand, if stronger, multiple scattering occurs, these photons may return to the amplification region and the amplified mode itself may consist of a multiple-scattering path. In random lasers, the conventional external cavity is absent, but light can be temporarily "trapped" inside the system, due to multiple scattering. Under suitable circumstances, the detrimental effects of diffuse scattering and other losses may be offset by the long path length of the photons within the gain region, giving rise to amplified laserlike emission.

The possibility of generation of amplified light by a randomly scattering medium with gain, first suggested by Letokhov [1], has received considerable attention recently [2–9]. Isotropic laser action has been observed in random colloidal suspensions [2,3] as well as optically [8] and electrically [9] pumped semiconductor powders. A dramatic narrowing of the spectrum and a shortening of the emission time [6] has been observed above a well-defined threshold in pump energy. Furthermore, recent experiments [10,11] have demonstrated, for the first time, that the emission of light from these random amplifying media is in fact coherent.

A great deal of experimental work [2–7] has been devoted to the phenomenon of lasing in paints that contain Rhodamine 640 dye molecules in methanol as gain media and a titanium oxide colloidal suspension as optical scatterers. Emission from these multiple-light-scattering dielectric microstructures exhibits spectral and temporal properties characteristic of a multi-mode laser oscillator, even though the system contains no conventional cavity mode. These so-called paint-on laser systems are of special interest for understanding emission in random media because the gain and scattering can be varied independently.

A number of attempts have been undertaken to develop theoretical models which are relevant to lasing in random media. The experimental observations on the emission properties can be partially explained by heuristic ring laser models [12]. A more microscopic and fundamental understanding of the spectrally resolved intensity input-output properties of the random laser have been provided by a simple diffusion model [13–15] for the average light intensity and a rate-equation description of the atomic excitation density. In the case of a purely one-dimensional light scattering model, this rate-equation picture has been improved by recourse to a more microscopic, time-dependent Maxwell-Bloch equation description [16].

The properties of the emission in photonic paints can be studied using a diffusion model [13] for optical scattering and transport. A diffusion model is adequate to study the random laser with nonresonant feedback [1] that occurs in the moderate scattering regime. In this case, wave interference does not play any role, and the optical feedback provided by the scatterers has the role to simply return the emitted photons to the active gain region of the system (rather than to an initial position), thereby stimulating further emission. In other words, it is intensity feedback. This is different from the case of a random laser with coherent feedback [8] operating in the strong scattering regime, where the recurrent scattering events lead to the formation of closed loops, acting as laser resonators. In the case of strong optical scattering, a more general model involving the electric field rather than the intensity of light is necessary to investigate the laser action. In the diffusion approximation, the propagation of light in the random amplifying medium is considered as an isotropic random walk. This is valid for the transport of light over distances large compared with the transport mean free path l^*, defined as the average distance the light travels in the

sample before its propagation direction is randomized. The diffusion approximation represents an approximation to the radiative transfer theory [17], which, in turn, is an approximation to the more general coherence propagation theory for the electric-field autocorrelation function [18]. The interaction between photons and molecules is treated by the Einstein rate equations for emission and absorption of light. The radiation emitted into the random amplifying medium is described by a set of diffusion equations, where the multiple-scattering character of the transport is described by a diffusion coefficient that replaces the cavity loss coefficient in a conventional laser. The properties of the gain medium enter the nonlinear diffusion equations through the gain coefficient. Previous results [13] show that a time-independent diffusion model entirely recaptures the experimentally observed average emission spectral properties for steady-state pumping with a large beam cross section. However, the different time scales of transport (which usually takes place on a picosecond time scale) and emission (taking place on a nanosecond time scale) processes in a random laser require a complete time-dependent model for the system dynamics. In this paper, we recapture both the emission spectrum and temporal response by solving the time-dependent nonlinear diffusion equations for emitted photons of different frequencies, for a pulsed pump field and for a narrow cross-section pump field. In addition, we retain the full time dependence of the Einstein rate equations rather than adiabatically eliminating the atomic degrees of freedom. For very short excitation pulses, it is not possible for the atoms to respond instantaneously to changes in the electromagnetic field. Our model is similar to the random walk model [15] used to study the lasing in photonic paints. For the pulsed pump, we consider both plane wave and Gaussian beam cross sections, and we find that the time-dependent diffusion model qualitatively recaptures the experimental results. In particular, our model describes how the laser threshold intensity varies with the transport mean free path and the pump beam cross section.

II. DIFFUSION MODEL

In amplifying random media, light is both multiply scattered and amplified. In laser paints, optical pumping brings the dye molecules to excited states. Through spontaneous emission, some excited molecules randomly emit photons. These photons travel in the medium, being scattered by titania particles and amplified by dye molecules, through stimulated emission. The emergent photon energy per unit time, unit solid angle, and unit interface area around the direction $\hat{\mathbf{k}}_f$ in the frequency range from ω to $\omega+d\omega$ and time t is then expressed in terms of the source intensity due to the spontaneous emission within the sample, $S_\omega(\mathbf{r}',t';\hat{\mathbf{q}})d\omega$ (energy per unit volume, per unit time, and per unit solid angle around direction $\hat{\mathbf{q}}$, in the frequency range from ω to $\omega+d\omega$). The output intensity also depends on the propagator $G_\omega(\mathbf{r}-\mathbf{r}',t-t';\hat{\mathbf{q}},\hat{\mathbf{k}}_f)$, which represents the number of photons per unit "volume" found at a position $\mathbf{r}$ at time t and traveling in a direction $\hat{\mathbf{k}}_f$, given a unit source intensity at position $\mathbf{r}'$ and time $t'<t$, emitting light in an initial direction $\hat{\mathbf{q}}$. This accounts for stimulated emission processes

$$I_{output}(\omega,\hat{\mathbf{k}}_f,t)d\omega=\frac{c}{4\pi l^{*3}}\int d\mathbf{r}\int d\mathbf{r}'\int dt'\int d\hat{\mathbf{q}} \times[S_\omega(\mathbf{r}',t',\hat{\mathbf{q}})d\omega] \times G_\omega(\mathbf{r}-\mathbf{r}',t-t';\hat{\mathbf{q}},\hat{\mathbf{k}}_f) \times\exp\left(-\frac{z}{|\hat{\mathbf{k}}_f\cdot\hat{\mathbf{z}}|l^*}\right). \tag{2.1}$$

The "volume" referred to above is assumed large compared to a cubic wavelength, so that both the "location" and wave vector of the photon can be approximately specified. The source intensity $S_\omega(\mathbf{r}',t';\hat{\mathbf{q}})$ is proportional to the density of excited molecules at position $\mathbf{r}'$ and time t' and their spontaneous-radiative-emission cross section at frequency ω and direction $\hat{\mathbf{q}}$. The Green's function $G_\omega(\mathbf{r}-\mathbf{r}',t-t';\hat{\mathbf{q}},\hat{\mathbf{k}}_f)$ describes the average propagation of photons through the gain medium from position $\mathbf{r}'$ at time t' with wave vector $(\omega/c)\hat{\mathbf{q}}$ to position $\mathbf{r}$ at time t and wave vector $(\omega/c)\hat{\mathbf{k}}_f$, involving the process of diffusion, absorption by unexcited dye molecules, and stimulated emission from excited dye molecules. Here, c is the speed of light, l^* is the transport mean free path of the emitted photons, and the factor $(c/4\pi l^{*3})\exp(-z/\hat{\mathbf{k}}_f\cdot\hat{\mathbf{z}}|l^*)d\mathbf{r}$ represents the fraction of the energy at $\mathbf{r}$ and time t that contributes to the emergent flux. The factor $\exp(-z/\hat{\mathbf{k}}_f\cdot\hat{\mathbf{z}}|l^*)$ represents the part of this energy which emerges from the output surface of the sample without being further scattered, amplified, or absorbed [19].

For random media in which scattering mean free path is very large compared to the wavelength, the propagation of light can usually be described as a diffusion process. Assuming an isotropic random walk process for both the emitted light and the pump light, the light propagation in the system is described by diffusion equations with appropriate absorption and gain terms, which depend on the local excitation of the dye molecules. In this case, it is convenient to introduce the propagator for the total intensity of light at frequency ω:

$$G_\omega(\mathbf{r},t)\equiv\int d\hat{\mathbf{q}}\int d\hat{\mathbf{k}}_f G_\omega(\mathbf{r},t;\hat{\mathbf{q}},\hat{\mathbf{k}}_f). \tag{2.2}$$

The diffusion equation for the emitted photons at frequency ω can be written as

$$\partial_t G_\omega(\mathbf{r}-\mathbf{r}',t-t')=D\nabla_{\mathbf{r}}^2 G_\omega(\mathbf{r}-\mathbf{r}',t-t')+\frac{c}{l_g(\omega,\mathbf{r},t)} \times G_\omega(\mathbf{r}-\mathbf{r}',t-t')+\delta(\mathbf{r}-\mathbf{r}')\delta(t-t'). \tag{2.3}$$

Here, $D=1/3cl^*$ is the classical diffusion constant, which is assumed not altered by the presence of the dye, and the gain coefficient of the dye solution, $l_g^{-1}(\omega,\mathbf{r},t)$, which is related to the absorption and stimulated emission processes in the system.

For a sample consisting of a slab of random gain medium with planar boundaries with air on either side, the boundary condition for Eq. (2.3) requires that the propagator vanish at "trapping planes" located at the distance $d=0.71\,l^*$, the "extrapolation length," outside the sample. This imposes the physical boundary condition that photons that come within a mean free path of the sample boundary leave the sample and are "absorbed" by the external environment, with no opportunity to reenter the random gain medium. This factor arises because the photon density cannot vanish at the sample surface. Photons diffuse out of the medium and must pass through the surface. The value of the "extrapolation length" may be obtained from the method of linear extrapolation [20].

It is useful to introduce the total intensity of light at frequency ω in terms of emitted local intensities:

$$I(\omega,\mathbf{r},t) \equiv c\int d\mathbf{r}'\int dt'\int d\hat{\mathbf{q}}[S_\omega(\mathbf{r}',t',\hat{\mathbf{q}})]G_\omega(\mathbf{r}-\mathbf{r}',t-t'). \tag{2.4}$$

This obeys the diffusion equation

$$\partial_t I(\omega,\mathbf{r},t) = D\nabla_{\mathbf{r}}^2 I(\omega,\mathbf{r},t) + \frac{c}{l_g(\omega,\mathbf{r},t)}I(\omega,\mathbf{r},t) + c\int d\hat{\mathbf{q}}S_\omega(\mathbf{r},t,\hat{\mathbf{q}}). \tag{2.5a}$$

Equation (2.5a) was obtained from the definition of $I(\omega,\mathbf{r},t)$ and the diffusion equation (2.3).

The propagation of the pump intensity in the medium is described by

$$\partial_t I_p(\mathbf{r},t) = D_p\nabla_{\mathbf{r}}^2 I_p(\mathbf{r},t) - \frac{c}{l_a(\mathbf{r},t)}I_p(\mathbf{r},t) + \frac{c}{l_p^*}I_{incident}(\mathbf{r},t), \tag{2.5b}$$

where $D_p=1/3cl_p^*$ is the diffusion coefficient for the pump intensity (l_p^* is the transport mean free path of the pump). For simplicity, we assume that the transport mean free path of the pump and emitted photons are the same ($D_p=D$). The absorption coefficient $l_a(\mathbf{r},t)$ depends on the density of dye molecules at position $\mathbf{r}$ and time t in the ground state and their absorption cross section at pump frequency. $I_{incident}$ represents the coherent incident pump intensity. Both the coherent ($I_{incident}$) and diffuse (I_p) parts of the pump intensity are assumed monochromatic and we suppress the frequency dependence of these fields in our discussion.

In the case of illumination by a plane wave propagating in the z direction, the system is homogeneous in the transverse directions, and we only consider the z dependence of the emitted and pump intensities. However, for a finite Gaussian pump beam cross section we make use of the cylindrical symmetry and write the gradients in the diffusion equations accordingly. In the first case, the boundary conditions for Eqs. (2.5a) and (2.5b) for a slab of thickness L are

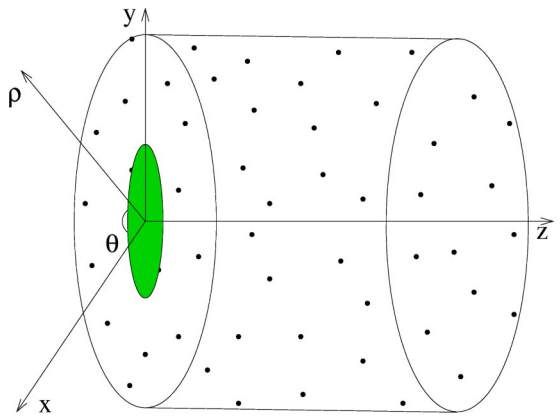

FIG. 1. Schematic view of the three-dimensional sample. A monochromatic pump beam of Gaussian cross section is incident from the left and is collimated in the direction perpendicular to $z=0$ plane (the shaded spot). The light intensity emitted from the front plane is measured by a detector on the left.

$$\begin{aligned} I(\omega,\mathbf{r},t)\big|_{\mathbf{r}\cdot\hat{\boldsymbol{z}}=-0.71l^*} &= I_p(\mathbf{r},t)\big|_{\mathbf{r}\cdot\hat{\boldsymbol{z}}=-0.71l^*} \\ &= I(\omega,\mathbf{r},t)\big|_{\mathbf{r}\cdot\hat{\boldsymbol{z}}=L+0.71l^*} \\ &= I_p(\mathbf{r},t)\big|_{\mathbf{r}\cdot\hat{\boldsymbol{z}}=L+0.71l^*} \\ &= 0. \end{aligned} \tag{2.6}$$

In the case of finite beam cross section, the sample itself is taken to have the shape of a cylindrical pill box of radius R and thickness L (see Fig. 1). In this case, an additional trapping surface is introduced to capture photons leaving the sample in the transverse direction:

$$I(\omega,\mathbf{r},t)\big|_{\mathbf{r}\cdot\hat{\boldsymbol{\rho}}=R+0.71l^*} = I_p(\mathbf{r},t)\big|_{\mathbf{r}\cdot\hat{\boldsymbol{\rho}}=R+0.71l^*} = 0. \tag{2.7}$$

Here, z and ρ are the cylindrical coordinates and the beam radius is considered less than the sample radius, R.

The proposed excitation scheme for laser dyes [13] is presented in Fig. 2. It consists of electronic levels with total spin zero (singlet states S_0, S_1) and total spin one (triplet states T_1, T_2), and an adjustable intersystem crossing rate between these states. Here, we neglect the intersystem crossing and consider that the emission dynamics corresponds only to the singlet state transitions, modeled as a standard four-level system. The lasing transition occurs between the third level (the lowest level in the S_1 manifold) and the second level (excited vibrational energy levels in the S_0 manifold). We further define the first level as the ground state in the S_0 manifold and the fourth level as an excited vibrational level of the S_1 manifold. The vibrational substructure included in our model provides an effective broadening of the essential states and is important for a quantitative comparison between our results and the experimentally observed line shape. The peak of the emission spectrum (obtained from the transition from the third level to the second level) is well separated from the absorption spectrum (obtained from the transitions from the first level to levels three and four). Accordingly, processes of stimulated emission from level 3 to level 1 and absorption from level 1 are ignored in comparison to the processes taking place between the lasing transition levels 3 and 2. Typical

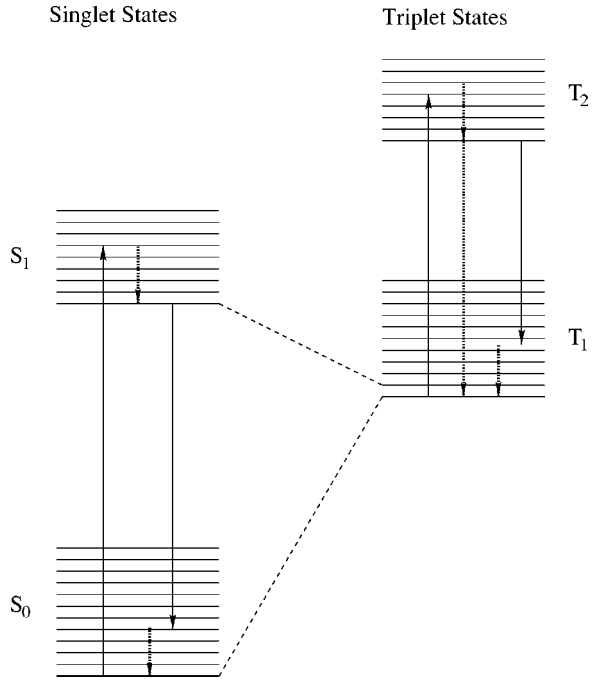

FIG. 2. Energy levels for a dye in solution. $S_0 \rightarrow S_1$ represents the pumping and absorption process, $S_1 \rightarrow S_0$ and $T_2 \rightarrow T_1$ represent the emission process, and $T_1 \rightarrow T_2$ represents the absorption process. The dotted lines represent the nonradiative decay processes, and the dashed lines represent the intersystem crossing process.

emitted photons do not have enough energy to excite the transitions from level one to the third and fourth levels. Furthermore, the populations in the fourth and second levels can be neglected due to the rapid nonradiative decays (on a time scale of 10^{-13} s) to the third and first levels, respectively. Therefore, one can neglect the reabsorption of the emitted radiation from level 2 to levels 3 and 4 and the transitions from level 4. As a result, the emission dynamics can be described by a single rate equation. The rate equation that describes the dye population per unit volume in the excited state (ground state of the S_1 manifold), N_2, reads

$$\frac{dN_2(\mathbf{r},t)}{dt} = P(\mathbf{r},t)N_0(\mathbf{r},t) - \Gamma_2 N_2(\mathbf{r},t) - \sum_{\omega} \sigma_e(\omega)\Phi(\omega,\mathbf{r},t)N_2(\mathbf{r},t). \tag{2.8}$$

Here, $N_0 = N - N_2$ is the population per unit volume in the ground state (N is the total density of dye molecules), P is the pumping rate, and $\Gamma_2 = \Sigma_\omega \Gamma_{21}(\omega)$ is the total decay rate of the lowest level of the S_1 manifold due to spontaneous emission into individual levels of S_0 with individual rates $\Gamma_{21}(\omega)$. Here $\sigma_e(\omega)$ is the stimulated emission cross section, corresponding to transitions between the bottom of the S_1 manifold and vibrational levels in S_0. Explicit forms of these functions are discussed in Sec. III. The photon flux $\Phi(\omega,\mathbf{r},t)$ (number of photons per unit area, per unit time) is related to the emitted light intensity through $\Phi(\omega,\mathbf{r},t) = I(\omega,\mathbf{r},t)/\hbar\omega$.

Recently [9] random laser action in rare-earth-doped nanopowders has also been reported. In such systems, the laser gain media generally consist of ionic species grown or doped within a host material. This is analogous to the organic dye laser, in which dye molecules are suspended in solvent. The solid-state dielectric lasers can be modeled as four-level systems, reducible, due to the rapid nonradiative decays, to two-level systems, entirely similar to the case of the dye molecules [21]. Therefore, the lasing in the rare-earth-doped nanopowders, with the powders playing the role of scatterers, is similar to the lasing in photonic paints. The formalism presented here can be straightforwardly applied to describe the emission properties of these alternative random amplifying media.

The pumping rate in Eq. (2.8) is given by

$$P(\mathbf{r},t) = \sigma_a(\omega_0)(\hbar\omega_0)^{-1} I_p(\mathbf{r},t). \tag{2.9}$$

Here, $\sigma_a(\omega_0)$ is the cross section of the singlet absorption at the pump frequency, ω_0.

The gain coefficient, the source intensity due to the spontaneous emission, and the absorption coefficient entering the diffusion equations are expressed in terms of dye population densities as

$$l_g^{-1}(\omega,\mathbf{r},t) \equiv \sigma_e(\omega)N_2(\mathbf{r},t), \tag{2.10a}$$

$$\int d\hat{\mathbf{q}} S_\omega(\mathbf{r},t,\hat{\mathbf{q}}) \equiv \hbar\omega\Gamma_{21}(\omega)N_2(\mathbf{r},t), \tag{2.10b}$$

$$l_a^{-1}(\mathbf{r},t) \equiv N_0(\mathbf{r},t)\sigma_a(\omega_0). \tag{2.10c}$$

It is convenient to rewrite the equations above in terms of dimensionless quantities. We define the dimensionless time $\tilde{t} \equiv t/t_a$ and the dimensionless length $\tilde{\mathbf{r}} \equiv \mathbf{r}/l_z$, where $t_a \equiv l_a^0/c$ and $l_z \equiv (l^* l_a)^{1/2}$ is the diffusion controlled extinction length; $l_a^0 \equiv [N\sigma(\omega_0)]^{-1}$ is a parameter in our model, related to the dye concentration. Here, we neglect saturation effects and approximate l_a by l_a^0 in the expression of the extinction length, but use the expression (2.10c) elsewhere. We also define the dimensionless intensities

$$\tilde{I}(\omega,\mathbf{r},t) \equiv \frac{c\sigma_{max}}{\hbar\omega\Gamma_2} I(\omega,\mathbf{r},t) \tag{2.11a}$$

and

$$\tilde{I}_p(\mathbf{r},t) \equiv I_p(\mathbf{r},t)/I_c, \tag{2.11b}$$

with $\sigma_{max} \equiv \max[\sigma_e(\omega)]$ and the characteristic intensity parameter $I_c \equiv \hbar\omega_0\pi^2\Gamma_2/\sigma_{max}$.

The set of nonlinear differential equations describing the system dynamics becomes

$$\partial_{\tilde{t}}\tilde{I}(\omega,\tilde{\mathbf{r}},\tilde{t}) = \nabla_{\tilde{\mathbf{r}}}^2\tilde{I}(\omega,\tilde{\mathbf{r}},\tilde{t}) + \frac{\sigma_e(\omega)}{\sigma_a(\omega_0)} n_2(\tilde{\mathbf{r}},\tilde{t})\tilde{I}(\omega,\tilde{\mathbf{r}},\tilde{t}) + \frac{\sigma_{max}}{\sigma_a(\omega_0)}\left[\frac{\Gamma_{21}(\omega)}{\Gamma_2} n_2(\tilde{\mathbf{r}},\tilde{t})\right], \tag{2.12a}$$

$$\partial_{\tilde{t}}\tilde{I}_p(\tilde{\mathbf{r}},\tilde{t}) = \nabla_{\tilde{\mathbf{r}}}^2\tilde{I}_p(\tilde{\mathbf{r}},\tilde{t}) - n_0(\tilde{\mathbf{r}},\tilde{t})I_p(\tilde{\mathbf{r}},\tilde{t}) + \frac{l_a^0}{l^*}\tilde{I}_{incident}(\tilde{\mathbf{r}},\tilde{t}), \tag{2.12b}$$

$$\frac{dn_2(\tilde{\mathbf{r}},\tilde{t})}{d\tilde{t}} = \frac{\Gamma_2 l_a^0}{c}\{\tilde{P}(\tilde{\mathbf{r}},\tilde{t})n_0(\tilde{\mathbf{r}},\tilde{t}) - [\tilde{R}_e(\tilde{\mathbf{r}},\tilde{t}) + 1]n_2(\tilde{\mathbf{r}},\tilde{t})\}. \tag{2.12c}$$

In Eqs. (2.12), $n_i \equiv N_i/N$ $(i=0,2)$ are the normalized dye populations, related to each other in our model through $n_0 = 1-n_2$,

$$\tilde{P}(\tilde{\mathbf{r}},\tilde{t}) \equiv P(\mathbf{r},t)/\Gamma_2 = \pi^2 \frac{\sigma_a(\omega_0)}{\sigma_{max}} \tilde{I}_p(\tilde{\mathbf{r}},\tilde{t}) \tag{2.13}$$

is the dimensionless pump rate, and

$$\tilde{R}_e(\tilde{\mathbf{r}},\tilde{t}) \equiv \left(\sum_\omega \sigma_e(\omega)\Phi(\omega,\tilde{\mathbf{r}},\tilde{t})\right)/\Gamma_2 = \int d\omega \frac{\sigma_e(\omega)}{\sigma_{max}} \tilde{I}(\omega,\tilde{\mathbf{r}}) \tag{2.14}$$

is the dimensionless stimulated-emission rate within the singlet manifold.

The boundary conditions for the diffusion equations are

$$\begin{aligned}\tilde{I}(\omega,\tilde{\mathbf{r}},\tilde{t})|_{\tilde{z}=-0.71l^*/l_z} &= \tilde{I}_p(\tilde{\mathbf{r}},\tilde{t})|_{\tilde{z}=-0.71l^*/l_z} \\ &= \tilde{I}(\omega,\tilde{\mathbf{r}},\tilde{t})|_{\tilde{z}=(L+0.71l^*)/l_z} \\ &= \tilde{I}_p(\tilde{\mathbf{r}},\tilde{t})|_{\tilde{z}=(L+0.71l^*)/l_z} \\ &= 0,\end{aligned} \tag{2.15}$$

together with

$$\tilde{I}(\omega,\tilde{\mathbf{r}},\tilde{t})|_{\tilde{\rho}=(R+0.71l^*)/l_z} = \tilde{I}_p(\tilde{\mathbf{r}},\tilde{t})|_{\tilde{\rho}=(R+0.71l^*)/l_z} = 0, \tag{2.16}$$

for the case of a finite cross-section pump beam.

Unlike previous studies [13], we treat the full time-dependent rate equation (2.12c) rather than carrying out an adiabatic elimination of the atomic degrees of freedom in favor of optical intensities. This more general treatment is useful in describing ultrashort-pulse excitations of the random medium.

For a slab in the *xy* plane illuminated by plane waves in the *z* direction, we can omit the *x* and *y* dependence and retain only partial derivatives with respect to *z* in the gradients in diffusion equations (2.12a) and (2.12b). In the case of a three-dimensional system, illuminated by Gaussian beam in the *z* direction, we assume a cylindrical symmetry of the system and use cylindrical coordinates. Neglecting the angular dependence, we make the substitution $\nabla^2_{\tilde{\mathbf{r}}} \to \partial^2_{\tilde{\rho}} + (1/\tilde{\rho})\partial_{\tilde{\rho}} + \partial^2_{\tilde{z}}$.

We introduce the homogeneously broadened output intensity

$$I_{out}(\omega,t) \equiv \int d\hat{\mathbf{k}}_f \int d\omega' I_{output}(\omega',t;\hat{\mathbf{k}}_f) g(\omega'-\omega), \tag{2.17}$$

where $g(\omega'-\omega)$ is the homogeneously (collision) broadened Lorentzian line-shape function [22], and I_{output} is defined in Eq. (2.1). We point out that in the more general case when the gain medium is both homogeneously and inhomogeneously broadened, the line-shape function $g(\omega'-\omega)$ is the composite Voigt line-shape function [22]. Finally, the total emergent photon energy from the medium (per unit area, per unit time, in the frequency range from ω to $\omega+d\omega$) is expressed as $I_{out}(\omega,t)d\omega$, where

$$\begin{aligned}I_{out}(\omega,t) = \frac{\hbar l_z^d \Gamma_2}{4\pi l^{*d}\sigma_{max}} \int d\hat{\mathbf{k}}_f \int d\omega' \int d\hat{\mathbf{r}} \\ \times \exp\left(-\frac{\tilde{z} l_z}{|\hat{\mathbf{k}}_f \cdot \hat{\mathbf{z}}| l^*}\right) \tilde{I}(\omega,\tilde{\mathbf{r}},\tilde{t})\omega' g(\omega'-\omega).\end{aligned} \tag{2.18}$$

Here, we use $d=1$ and $\int d\hat{\mathbf{r}} \to \int_0^{L/l_z} d\tilde{z}$ for a one-dimensional model, and $d=3$ and $\int d\hat{\boldsymbol{r}} \to 4\pi \int_0^{R/l_z} \tilde{\rho} d\tilde{\rho} \int_0^{L/l_z} d\tilde{z}$, for the three-dimensional model with finite pump beam cross section.

In order to calculate the output intensity, we solve the system of diffusion and rate equations (2.12). This provides us with all the information on the spectral, spatial, and temporal properties of the emitted intensity, as well as the gain coefficient inside the sample. By approximating the integral in Eq. (2.14) by a sum over a set of discrete frequencies ω_i, $i=1,2,\ldots,N$, this system transforms to a set of $N+3$ coupled nonlinear partial differential equations, which can be solved numerically using the method of lines [23]. This method is based on replacing the spatial (boundary value) derivatives with an algebraic approximation over a spatial grid. The resulting system of initial-value ordinary (time-dependent) differential equations (ODE's) is then integrated numerically, using an established ODE code.

III. NUMERICAL RESULTS FOR EMISSION INTENSITY AND LASING THRESHOLD

We solve the set of diffusion and rate equations (2.12) for different values of scatterer density, dye concentration, and pump intensity, both for plane-wave pump beams,

$$I_{incident}(\mathbf{r},t) = I_0 \sqrt{\frac{a}{\pi}} \exp(-z/l_z) \exp\left[-a\frac{(t-t_0-z/c)^2}{\tau_p^2}\right], \tag{3.1}$$

and for pump beams with Gaussian cross sections,

$$\begin{aligned}I_{incident}(\mathbf{r},t) = I_0 \sqrt{\frac{a}{\pi}} \exp(-z/l_z) \\ \times \exp\left[-a\frac{(t-t_0-z/c)^2}{\tau_p^2}\right] \exp[-a(\rho/\rho_p)^2].\end{aligned} \tag{3.2}$$

Here I_0 is the pump intensity, $a = 4\ln 2$, t_0 is the time at which the maximum of the pump is incident on the sample surface, and τ_p is the pulse temporal profile, full width at half maximum. ρ_p is the pulse radial profile, full width at half maximum.

The stimulated emission cross section used is given by the expression [21]

$$\sigma_e = \frac{2\pi^2}{3\epsilon_0 c\hbar}\int d\nu \mathcal{D}(\nu)|\mu|^2 g(\omega-\nu)\nu. \tag{3.3}$$

Here, ε_0 is the vacuum permittivity, $D(\nu)$ is the rovibrational density of state of the relevant energy band of the dye, and μ is the transition matrix element of the electric dipole moment. We assume that

$$\mathcal{D}(\nu)|\mu|^2 \propto e^{-|a(1-\nu/\omega_0)|}[1+b(1-\nu/\omega_0)^2]. \tag{3.4}$$

Here, $[1+b(1-\nu/\omega_0)^2]$ describes the degeneracy of the excited vibrational states, and $e^{-|a(1-\nu/\omega_0)|}$ is the Frank-Condon overlap factor [21] for the dipole matrix element connecting the ground states and the excited electronic state in different vibrational states. a, b, and ω_0 are three parameters, adjusted in order to fit experimental data on the peak position and the linewidth of the fluorescence spectrum (emission cross section) of the dye molecules. The values $a=35$, $b=264$, and $2\pi c/\omega_0=615$ nm have been used in the calculations [13]. The spontaneous emission rate $\Gamma_{21}(\omega)$ is related to $\sigma_e(\omega)$ through the relation between the Einstein A and Einstein B coefficients [21]. In the following calculations, we choose $\sigma_a(\omega_0)/\sigma_{max}=2$, the spontaneous emission decay rate is set to $\Gamma_2=1$ ns, the sample thickness and radius are $L=1$ cm and $R=1$ cm, respectively, and the parameter l_a^0 is calculated using the fact that the pump penetration depth of a $2.5\times10^{-3}M$ dye solution is about 50 μm [2]. The homogeneously broadened line-shape function is expressed as

$$g(\omega-\omega') = \frac{1}{\pi}\frac{\Delta\omega}{(\omega-\omega')^2+(\Delta\omega)^2}, \tag{3.5}$$

with $\Delta\omega=(2\pi c/\lambda_0)(6\text{ nm}/2\lambda_0)$, where $\lambda_0=620$ nm. The 6-nm linewidth is chosen since it is the minimum width to which the emission narrows under strong laserlike amplification. This value of the homogeneous linewidth of the gain medium is close to that experimentally observed for similar systems [24,25].

We begin by presenting the results obtained for plane-wave excitations (3.1), with pulse duration $\tau_p=10$ ps, as reported in some of the experiments [6]. This requires solving the one-dimensional diffusion equations, coupled to the atomic rate equation.

Figure 3 shows the emission spectrum at different pump intensities, for fixed dye concentration and scatterer density. The spectral and temporal response of the system to the pump pulse is presented in Fig. 4, which shows the emitted pulse linewidth and duration as function of pump intensity. The shapes of these curves are consistent with the experimental observations. We see from Fig. 4 that there exists a well-defined value of the pump intensity above which the emission characteristics from the disordered medium change dramatically: the linewidth is narrowed and the emission shortens dramatically and reaches its peak value at earlier times. As in experiments, the threshold intensity appears to be the same for both spectral and temporal emission properties. Also, as experimentally observed, it is obtained that, above the threshold, the emission at the peak wavelength increases more rapidly with the pump intensity than it does

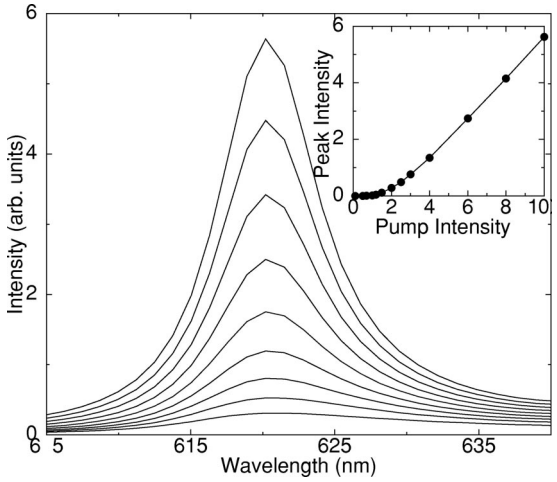

FIG. 3. The emission spectrum at different values of peak pump intensity, varying from 0.5×10^7 J cm^{-2} s^{-1} (the innermost curve) to 10×10^7 J cm^{-2} s^{-1} (the outmost curve), for a 10-ps plane-wave pulse. The transport mean free path is set to 6.2×10^{-4} cm, and the dye concentration is $2.5\times10^{-4}M$. Here the entire cross section of the sample is illuminated uniformly. The inset shows the variation of the peak intensity with the pump intensity, for the same set of sample parameters.

below the threshold. This is shown in the inset in Fig. 3, where we plot the emission intensity at the peak wavelength (620 nm) as a function of pump intensity.

The lasing in the random medium is enhanced rather than hindered by multiple-light-scattering processes in the system. The lasing threshold in fact decreases with the scatterer density. We see from Fig. 5 that the threshold intensity, here defined as the pump intensity for which the duration of the emitted pulse is 100 ps (which from Figs. 3 and 4 is also the pump intensity for which the emission spectral linewidth collapses and the slope of the input-output curve changes), de-

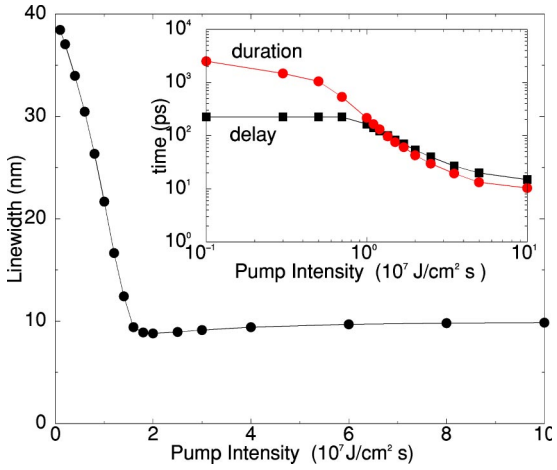

FIG. 4. Spectral linewidth as a function of peak pump intensity. The pulse characteristics, transport mean free path, and dye concentration are the same as in Fig. 3. The inset shows the dependence of the pulse duration and the time delay of the peak emission with respect to the peak pump excitation on the peak pump intensity, for the same set of sample parameters.

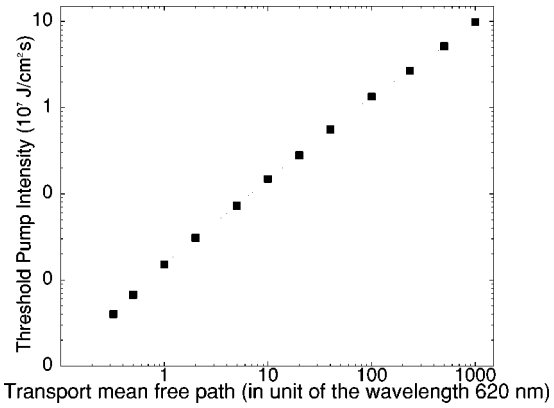

FIG. 5. Variation of the threshold intensity with the transport mean free path. The dye concentration is set equal to $2.5\times10^{-4}M$, and the sample parameters are the same as in Fig. 3.

creases when the transport mean free path decreases (or, equivalently, as the scatterer density is increased).

In Fig. 6, we plot the temporal profile of the emitted pulse and its spectral linewidth, for a pump intensity above the threshold value, and Fig. 7 shows the excited-state population at the same value of the pump intensity.

Experimental studies [7] have also demonstrated the strong dependence of the threshold pump intensity on the spot size of the incident pump pulse. In the case of illuminating the sample with a beam of finite cross section, the lasing threshold has been found to increase by 70 times as the excitation spot diameter was gradually decreased from 20 to below 5 transport mean free paths [7]. We demonstrate that this is the result of multiple light scattering. For a large excitation area, the pumped volume is large and the emitted photons will spend more time in this amplifying region. For a small excitation volume, the emitted light, which propagates diffusively through the sample, will leave the amplifying region after a short time. In the latter situation, a higher pumping level is necessary to achieve positive gain in the

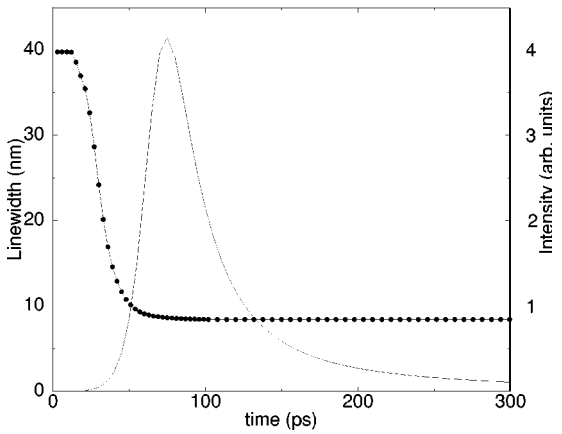

FIG. 6. Temporal emission profile for the same sample parameters as in Fig. 5 and incident peak pump intensity of 3×10^{7} J cm^{-2} s^{-1}. The dots show the time ependence of the spectral linewidth of this pulse, at the same value of the peak pump intensity. The time $t=0$ corresponds to the time when the peak of the pump excitation enters the sample.

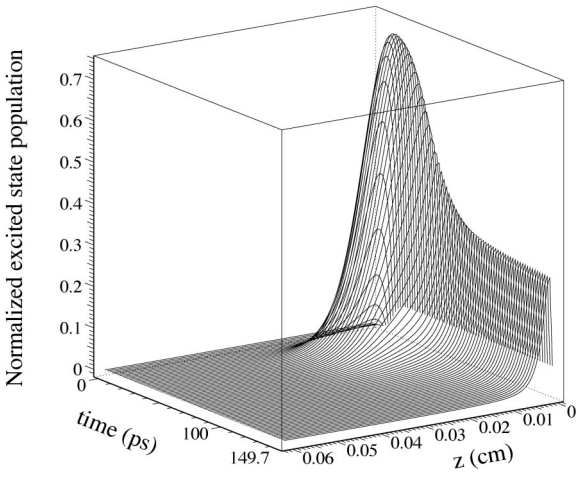

FIG. 7. Normalized excited-state population for the same sample and pump intensity as in Fig. 6.

system. We study this effect in the framework of a more complete, three-dimensional diffusion model. Although the main ideas behind this approach remain the same as in the one-dimensional case, the extension of the diffusion model to three dimensions involves significantly more effort in terms of numerical analysis and programming. For simplicity, the atomic rate equations are solved under "quasi-steady-state" conditions, by putting $dn_2/dt=0$ in the rate equation (2.12c). This quasi-steady-state atomic response is then substituted into the time-dependent diffusion equation. In doing so, we assume that both the emitted intensity and the pump intensity vary much more slowly in time than the atomic variables. The solutions for the atomic populations obtained this way are not truly constant, but are determined by the instantaneous values of these slowly varying field variables. As discussed in Sec. IV, this approach does not provide an accurate description of the dynamics of the system, and we will use it only to calculate the emission spectrum. This is enough to investigate the effect of the transverse diffusion on the lasing threshold.

We consider a Gaussian beam cross section of the form (3.2), with a duration of $\tau_p=10$ ns, and investigate the dependence of the threshold intensity on the radial full width at half maximum, ρ_p. The result is obtained for a set a sample parameters as those used in the experiments [7]. Here the threshold intensity is obtained from a plot of the spectral linewidth as a function of pump intensity, as shown in Fig. 8, and represents the intensity at which the linewidth collapses. We see from Fig. 9 that the lasing threshold intensity dramatically decreases when the excitation spot diameter increases above a few transport mean free paths, corresponding to a larger gain volume. This result is in quantitatively very good agreement with the experimental findings.

IV. PHYSICAL INTERPRETATION OF TEMPORAL BEHAVIOR

We now discuss qualitatively the necessity of a nonadiabatic time-dependent model in order to fully recapture the

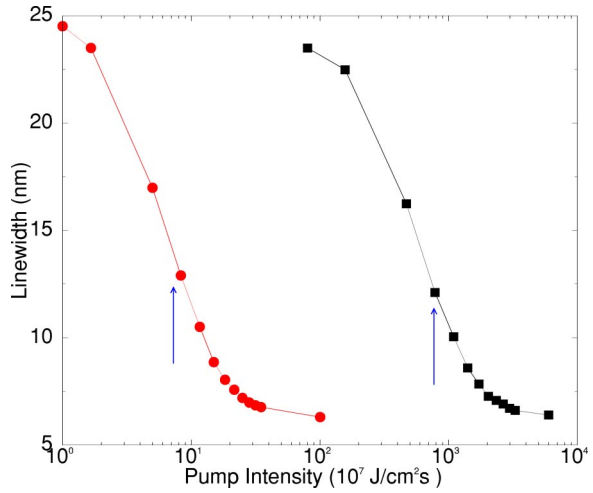

FIG. 8. Emission linewidth vs pump intensity for pump diameters of 2 mm (circles) and 100 μm (squares). The up-arrow indicates the position of the threshold. The sample thickness and radius are each set to 1 cm, and the dye concentration and transport mean free path are set to 10^{-3} mol/l and 10^{-2} cm, respectively, in the calculation. For an absorption cross section $\sigma_a = 1.6 \times 10^{-16}$ cm^2, 10^{-3} mol/l dye concentration corresponds to an absorption length of 10^{-2} cm.

dynamics of the system. The temporal profiles of the emitted pulse and excited-state population, as well as the threshold behavior of the emitted pulse duration, are important features of any laser. However, the characteristic time scales of these features depend on the specific system. In what follows, we employ a simplified rate equation model for both atoms and photons, to interpret our results on the temporal response of the random laser.

In a random laser, the majority of the emitted intensity arises from a region $0 \leqslant z \leqslant l_z$ within the diffusion-controlled extinction length, where significant population inversion is achieved. The pump pulse only reaches this region, where it is absorbed by the dye molecules and scattered by titania

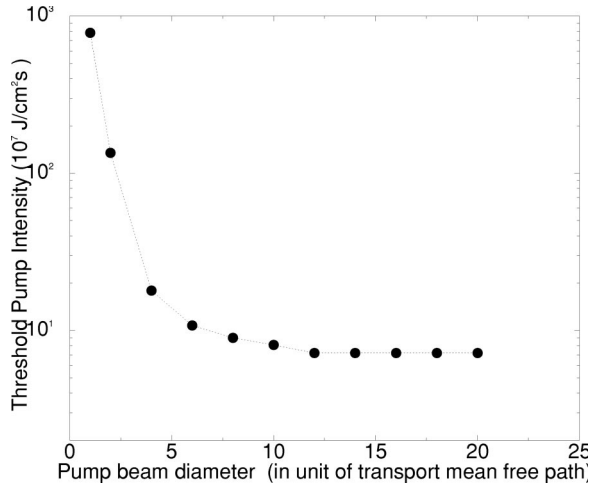

FIG. 9. Variation of the threshold intensity with the pump-beam diameter in units of transport mean free path, $l^* = 0.01$ cm. The other sample parameters are the same as for Fig. 8.

particles. Based on this fact, in our analysis, the real slab is replaced by an "effective slab" of thickness l_z. The general solution for the emitted intensity for the one-dimensional slab geometry [Eq. (2.5a)] can then be expressed as an expansion in the "eigenfunctions" of the diffusion equation for this effective domain,

$$\partial_z^2 \psi_k(z) = E_k \psi_k(z), \tag{4.1}$$

as

$$I(\omega,z,t) = \sqrt{\frac{l_z}{2}} \sum_{k \geqslant 1} n_k(\omega,t) \psi_k(z). \tag{4.2}$$

Here, $\sqrt{(2/l_z)}\psi_k(z) = \sin(k\pi z/l_z)$. We point here that this represents only a heuristic approach, necessary to identify the time scale corresponding to diffuse photon propagation in the amplifying medium. Strictly speaking, the diffusion approximation becomes inapplicable as the physical length scale of the system becomes comparable to the transport mean free path, and surface corrections have to be considered. To obtain a qualitative picture, we keep only the first term in the expansion (4.2). Using this expression for the emitted intensity, the diffusion equation (2.5a) becomes

$$\partial_t I(\omega,z,t) = -\gamma_c I(\omega,z,t) + c\sigma_e(\omega) N_2(z,t) I(\omega,z,t) + c\hbar\omega\Gamma_{21}(\omega) N_2(z,t). \tag{4.3}$$

Here, $\gamma_c \equiv \pi^2 D/l_z^2$ is the "cavity" decay rate, and we have used expressions (2.10a) and (2.10b) for the gain coefficient $l_g(\omega,z,t)$ and the source intensity due to spontaneous emission, $S_\omega(z,t,\hat{\mathbf{q}})$, respectively. For a random laser characterized by values of the transport mean free path and absorption length as those used in the calculations in Sec. III, the cavity decay constant γ_c corresponds to a decay time of picoseconds. The slow response of the atomic system compared to the light transport is a characteristic of the random lasers and leads to relaxation oscillations (laser spiking) in the dynamic response of the system at the threshold crossing. A detailed study of this regime is presented in [14,26,27].

We further divide Eq. (4.3) by $c\hbar\omega$ and sum over frequencies to arrive at the equation

$$\dot{n} = -\gamma_c n + \kappa n N + \Gamma N. \tag{4.4}$$

Here, $n(z,t) \equiv c^{-1}\Sigma_\omega \Phi(\omega,z,t)$ is the total number of photons per unit volume in the system, $N \equiv N_2(z,t)$ is excited-state population density, and $\Gamma \equiv \Gamma_2$. For simplicity, we omit the dependence on the spatial coordinate z hereafter. In deriving Eq. (4.4), we have used that the laser emission spectrum is usually much narrower than the spontaneous emission spectrum and made the approximation

$$\sum_\omega \sigma_e(\omega)\Phi(\omega,z,t) \approx \sigma_e^{max} \sum_\omega \Phi(\omega,z,t), \tag{4.5}$$

such that $\kappa \equiv c\sigma_e^{max}$.

Similarly, the rate equation (2.8) for the excited-state population can be rewritten as

$$\dot{N} = P - \kappa n N - \Gamma N, \tag{4.6}$$

where $P \equiv P(z,t)N_0(z,t)$. For simplicity, in the analysis presented here, we neglect pump diffusion. We note that Eqs. (4.4) and (4.6) are similar to the rate equations of a conventional laser.

First, consider the case in which the laser is operating below or near threshold. In this case, the number of photons in the system is very small, and the stimulated emission terms in Eqs. (4.4) and (4.6) can be neglected. During the course of a picosecond pump pulse exciting the system, the atomic population builds up rapidly towards a maximum value, and spontaneous emission (which takes place on a nanosecond time scale) does not yet contribute to the system dynamics. Atomic population decay by spontaneous emission occurs only after the passage or extinction of the pump. As a consequence, the temporal profile of the excited-state population for the dye molecules exhibits a rapid buildup and slow decay, with an overall width on the scale of nanoseconds. The emitted pulse temporal profile has similar characteristics. When the excited population is below a threshold value, $N_{th} \approx \gamma_c/\kappa$, the number of photons in the system remains very small. As soon as the number of excited molecules passes through the threshold value, the laser gain exceeds the loss, and the number of photons begins to increase exponentially. The exponential buildup rate is $\gamma_c' \equiv \gamma_c(N(t)/N_{thr}-1) \approx \gamma_c$. The buildup time of the number of photons is of the order of the cavity decay time, which has the value on the scale of picoseconds for a typical random laser. The increase of the photon number continues as long as the population inversion is above the threshold value. During this time, the population inversion increases to the maximum value (on a time scale of picoseconds, as discussed above) and then slowly decreases (on a nanosecond time scale) to the threshold value. The point in time at which the population inversion returns to its threshold value coincides with the time (t_{peak}) where the photon number reaches its peak value (n_{peak}). Therefore, the buildup time for the emitted radiation is on the order of hundreds of picoseconds to nanoseconds. The subsequent decrease in photon number takes place on a nanosecond time scale. As a consequence, the emission pulse duration is of the order of nanoseconds. The decay rate of the emission can be obtained using the solution of Eq. (4.4), integrated from the moment the photon number reaches maximum value, and where we neglect the stimulated emission term:

$$n(t) = (n_{peak} - A)e^{-\gamma(t-t_{peak})} + Ae^{-\Gamma(t-t_{peak})}, \tag{4.7}$$

where

$$A = \frac{\Gamma}{\gamma_c - \Gamma} N_{thr} e^{-\Gamma t_{peak}} \approx \frac{\Gamma}{\gamma_c} N_{thr} e^{-\Gamma t_{peak}}. \tag{4.8}$$

Here, we have used that for the time interval considered $N(t) = N_{thr}\exp(-\Gamma t)$. From Eq. (4.7) we also notice that the exponential decay of the emission exhibits a fast component, corresponding to the cavity decay, and a slow component, corresponding to the spontaneous emission.

Consider now the case when the laser is operating well above threshold. Under the action of the pump, the number of molecules in the excited state increases on a time scale of picoseconds (the pulse duration). However, due to the presence of a large number of photons in the system, the stimulated emission becomes dominant and leads to a much faster decay of the population inversion after reaching the maximum value. This decay rate is larger than the spontaneous emission rate by a factor equal to the number of photons in the system (the stimulated emission rate). Since the emission buildup time is equal to the time the population inversion reaches the maximum value, we obtain the picosecond scale delay for the emission above threshold. The fast decay of the population inversion leads, in turn, to a fast decay of photon number. This can be seen using the formal solution of the photon rate equation (4.4) for the case of laser operating above threshold, obtained by replacing γ_c by γ_c', and $\exp(-\Gamma t)$ with $\exp(-n\Gamma t)$ [using $N(t) = N_{thr}\exp(-n\Gamma t)$]. As a result, the emission pulse duration is in the range of picoseconds. Moreover, the fact that the pulse duration is inversely proportional to γ_c' and $n\Gamma$ (which, in turn, are proportional to the pump rate) explains its threshold behavior. Namely, the emitted pulse duration decreases with increasing pump rate, until (for large values of the pump) it reaches a saturation value equal to cavity decay rate. Similarly, the emission time delay has a component that is inversely proportional $n\Gamma$, which also exhibits a threshold behavior mirroring the threshold behavior of the number of emitted photons. Also, the transient gain narrowing, presented in Fig. 6, is related to the increase of the emitted intensity with time, since, according to Schawlow-Townes formula [21], the spectral linewidth is inversely proportional to the number of emitted photons.

We note that the emission pulse exhibits a fast decay followed by a slow decay for the random laser operating above threshold. When the emitted laser pulse leaves the sample and stimulated emission becomes negligible, the temporal decay of the residual atomic population inversion occurs by spontaneous emission. This slow decay of the population inversion leads to a tail in the emission, similar to the case of the laser operating below threshold. However, this low intensity tail does not substantially alter the emitted pulse duration, since it is acquired only after the number of photons decreases dramatically.

A consequence of the interpretation provided above is the importance of the nonadiabatic atomic response. While a model in which the atomic variables are adiabatically eliminated [13] is adequate to describe steady-state spectral emission properties, it cannot recapture important features of the emitted pulse. By adiabatically eliminating the atomic variables, one forces the atomic population to instantaneously follow the pump. Consequently, the temporal profile of the emitted light will be dictated by the excitation, regardless of whether the laser operates below or above threshold. In this case, the threshold behavior of the emitted pulse duration and delay (presented in Fig. 4) will be lost. This can easily be seen if we solve Eq. (4.6) under steady-state condition and substitute the resulting population inversion into Eq. (4.4):

$$\dot{n} = -\gamma_c n + P(t). \tag{4.9}$$

Clearly, the number of emitted photons will simply increase in time with the pump intensity and then decrease at a rate

equal to the cavity decay rate, irrespective of the lasing threshold.

V. CONCLUSIONS

In summary, we have demonstrated the ability of the diffusion model with nonlinear, nonadiabatic atomic coupling to recapture the experimentally observed spectral and temporal properties of the emission in photonic paints. Most of the important lasing features, such as the narrowing of the spectrum, shortening of the emitted pulse, and the linear input-output for pump intensities above a threshold value, can be accurately recaptured using a one-dimensional time-dependent diffusion model. A three-dimensional diffusion model is required to describe effects where the excitation spot size and the gain volume is limited, and significant diffusion of photons out of the gain region occurs prior to the buildup of the emitted pulse.

The analysis presented here assumes a white-noise model for the disorder and considers only isotropic scattering with a uniform distribution of active molecules. It would be of considerable interest to extend this study to the case of more general types of anisotropic scattering and nonuniform dye concentration. It is possible that the statistical and spatial distribution of the gain material will influence the diffusion coefficient [28] and thereby affect the lasing properties. It is also of considerable interest to study the influence of more detailed properties of the scattering microstructures on lasing properties. For example, with finite-size scatterers which have some form of spatial correlation, the scattering is anisotropic. In this case, there is a distinction between the scattering mean free path for photons, l, and the transport mean free path l^*. Such a situation will require the generalization of the multiple-light-scattering theory for a passive random medium [18] in the case of a nonlinear active random medium, characterized by a complex, intensity-dependent dielectric function. A more fundamental multiple-light-scattering model with nonlinear gain may also be crucial to describing the very strong scattering regime of incipient photon localization ($l^* \leqslant \lambda$) [29]. In this regime, our simple diffusion model suggests the likelihood for dramatic enhancements in the laserlike response of the random medium.

ACKNOWLEDGMENT

This work was supported in part by the Natural Sciences and Engineering Research Council of Canada.

[1] V. S. Letokhov, Zh. Eksp. Teor. Fiz. **53**, 1442 (1967) [Sov. Phys. JETP **26**, 835 (1968)].
[2] N. M. Lawandy *et al.*, Nature (London) **368**, 436 (1994).
[3] W. L. Sha, C.-H. Liu, and R. R. Alfano, Opt. Lett. **19**, 1922 (1994).
[4] D. S. Wiersma, M. P. van Albada, and Ad. Lagendijk, Nature (London) **373**, 203 (1995).
[5] N. M. Lawandy and R. M. Balachandran, Nature (London) **373**, 204 (1995).
[6] M. Siddique, R. R. Alfano, G. A. Berger, M. Kempe, and A. Z. Genack, Opt. Lett. **21**, 450 (1996).
[7] G. van Soest, Makoto Tomita, and A. Lagendijk, Opt. Lett. **24**, 306 (1999).
[8] H. Cao, Y. G. Zhao, S. T. Ho, E. W. Seelig, Q. H. Wang, and R. P. H. Chang, Phys. Rev. Lett. **82**, 2278 (1999).
[9] G. R. Williams, S. B. Bayram, S. C. Rand, T. Hinklin, and R. M. Laine, Phys. Rev. A **65**, 013807 (2002).
[10] G. Zacharakis, N. A. Papadogiannis, G. Filippidis, and T. G. Papazoglou, Opt. Lett. **25**, 923 (2000).
[11] H. Cao, Y. Ling, J. Y. Xu, C. Q. Cao, and P. Kumar, Phys. Rev. Lett. **86**, 4524 (2001).
[12] R. M. Balachandran, N. M. Lawandy, and J. A. Moon, Opt. Lett. **22**, 319 (1997).
[13] S. John and G. Pang, Phys. Rev. A **54**, 3642 (1996).
[14] D. S. Wiersma and A. Lagendijk, Phys. Rev. E **54**, 4256 (1996).
[15] G. A. Berger, M. Kempe, and A. Z. Genack, Phys. Rev. E **56**, 3462 (1997).
[16] X. Jiang and C. M. Soukoulis, Phys. Rev. Lett. **85**, 70 (2000).
[17] K. M. Case and P. W. Zweifel, *Linear Transport Theory* (Addison-Wesley, Reading, MA, 1967).
[18] S. John, G. Pang, and Y. Yang, J. Biomed. Opt. **1**, 180 (1996).
[19] E. Akkermans, P. E. Wolf, and R. Maynard, Phys. Rev. Lett. **56**, 1471 (1986).
[20] A. M. Weinberg and E. P. Wigner, Physical *Theory of Neutron Chain Reactors* (University of Chicago, Chicago, 1958).
[21] O. Svelto and D. C. Hanna, *Principles of Lasers* (Plenum, New York, 1989).
[22] R. Loudon, *The Quantum Theory of Light* (Oxford University Press, Oxford, 2002).
[23] N. K. Madsen and R. F. Sincovec, ACM Trans. Math. Softw. **5**, 236 (1979); J. G. Bloom, R. A. Trompert, and J. G. Verwer, *ibid.* **22**, 302 (1996).
[24] A. Elschner, L. R. Narasimhan, and M. D. Fayer, Chem. Phys. Lett. **171**, 19 (1990).
[25] At room temperature, the homogeneous linewidth of Rhodamine B in ethanol is ~2.5 nm [24]. In this case, for the sample parameters used in Fig. 4, the emission spectral linewidth above threshold is ~6.5 nm (the emission natural linewidth being ~4 nm, as also suggested by the results presented in Fig. 4), close to the experimentally observed value.
[26] G. van Soest, F. J. Poelwijk, R. Sprik, and A. Lagendijk, Phys. Rev. Lett. **86**, 1522 (2001).
[27] C. M. Soukoulis, X. Jiang, J. Y. Xu, and H. Cao, Phys. Rev. B **65**, 041103 (2002).
[28] K. Busch (unpublished).
[29] S. John, Phys. Rev. Lett. **53**, 2169 (1984).